PROPERTIES OF PRINTED MESH ANTENNAS

L. Shafai* and W. Chamma**
*Department of Electrical and Computer Engineering
University of Manitoba
Winnipeg, Manitoba, Canada R3T 5V6
**InfoMagnetics Technologies Corporation
Winnipeg, Manitoba, Canada R2J 3T4

1. Introduction

In some applications a planar antenna system is required to operate in two or several widely separated frequency bands, and in each band in two linear or circularly polarized modes. Often the required gain is large and an antenna array must be utilized. When a beam scanning is not required the implementation becomes simpler. However, with a requirement of beam scan the problems associated with grating lobes, and active device incorporation in the feed network, complicate the antenna element selections and their collocation in the array environment. Stacking the array elements of different frequency bands, using multiple substrates, facilitates implementation but is useful when the upper frequency elements can be stacked on the lower frequency ones. The reverse problem is impractical, when the larger low frequency elements must be placed over the smaller patches. This problem manifests when the bandwidth requirement of the low frequency band is large and the element must be raised to a considerable height over the ground plane, or its frequency is excessively lower than that of the upper band, again causing relatively large separations. In such cases and to prevent the blockage of upper frequency radiation, a mesh antenna at the lower band may be utilized. While its configuration resembles a microstrip patch, it behaves differently. Some of its properties are investigated in this paper.

2. Mesh antenna

Fig. 1 shows the geometry of a possible dual band, dual polarized array configuration. The low frequency element is an L-Band probe fed mesh antenna and the upper band element is a conventional square patch. For these bands, the frequency ratio is about 4 and an array unit cell consists of a single L-Band element with sixteen C-Band patches. Also, for nearly equal bandwidths at both bands the L-Band substrate becomes considerably thicker and a mesh type antenna is a useful choice. To reduce the array weight honeycomb substrates are used for both bands.

In this configuration the L-Band element is above the C-Band patches, and a solid patch can not be used. The mesh geometry allows the radiation of C-Band elements, but nevertheless influences their characteristics. For best design, i.e. small interaction between the elements of two bands, the L-Band antenna should not physically block the C-Band elements. However, in practice the frequency ratio may be arbitrary, and also the size and separation of the C-Band elements depend on the frequency and the array scan range. This means, the size of the L-Band element can not be arbitrary. In other words, for a given C-Band array configuration, one may require a tuning capability for the L-Band element to design a resonant antenna, while maintaining a suitable

physical size and shape. Note that, in Fig. 1. both antenna types are fed by a symmetric balanced feed to minimize cross-polarization.

Mesh type printed antennas have been investigated previously. Andrasic and James [1] have considered mesh type patches as a dichroic radome over a high frequency patch. In their design the mesh cell size was too small, with respect to the wavelength, and did not influence its properties significantly. Other investigators have considered different configurations. Conti et al. [2] have presented a wire grid microstrip antenna and investigated its array performance. A more detailed analysis of this antenna was recently investigated by Nakano et al [3], where a double layer grid antenna for dual polarization was also introduced.

The geometry presented in this study differs from the earlier ones in that, the mesh itself is a resonant structure. In a simple term, it can be seen as a combination of a loop and cross-dipole antenna. As such its, resonance and bandwidth are influenced by the parameters of these sub-elements. They also affect its cross-polarization. The combination acts as a quasi-huygen source, reducing its cross-polarization. It is therefore a tunable antenna with superior electrical properties.

3. Results

For a given substrate height, the mesh antenna has three physical parameters of the outside rim width, the width of its central cross and the location of its feeds. It was found that all these three parameters strongly influence the resonant frequency and bandwidth of the antenna. It can be analyzed by a suitable moment method. However, since in the present case honeycomb substrate is used a simple wire model is utilized, and found to be quite accurate. Sample of calculated results are shown in Figs. 2 to 6. In Fig. 2. the computed current magnitude, shown as arrows, are superimposed on the wires, and show the complete isolation of the orthogonal polarization feeds. Figs 3 and 4 show the input impedance and its Smith Chart plot, while Fig. 5 shows the radiation patterns. A sample antenna was also fabricated and tested. Its measured return loss S_{11} is shown in Fig. 6, with a -10dB bandwidth of about 7%. It was found that, the resonance frequency can easily be controlled by the above mentioned parameters. The detail of the study will be provided during the presentation.

4. References

[1] G. Andrasic and J.R. James, "Investigation of Superimposed Dichroic Microstrip Antennas", *Fifth Int. Conf. on Antennas & Propagation ICAP87*, Pt. 1, pp. 485-488, U. of York, UK, 1987.

[2] R. Conti, J. Toth, T. Dowling and J. Weiss, "The Wire Grid Microstrip Antenna", *IEEE Trans.* Vol. AP-29, No. 1, pp. 157-166, 1981.

[3] H. Nakano, I. Oshima, H. Mimaki, K. Hirose and J. Yamauchi, "Centre-Fed Grid Array Antennas", *IEEE Symposium*, Vol 4, pp. 2010-2013, Newport Beach, 1995.

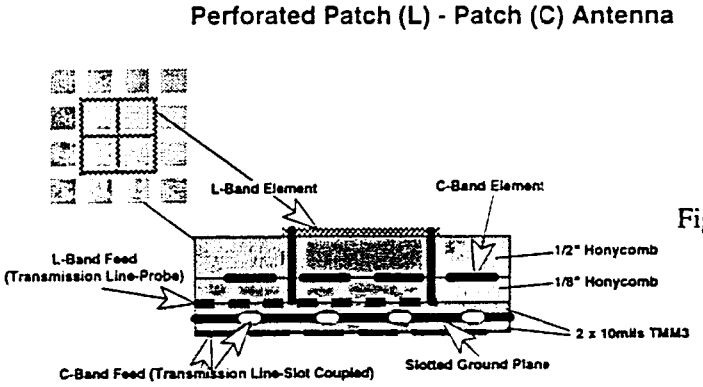

Fig. 1 Configuration of a dual-band dual polarized antenna array.

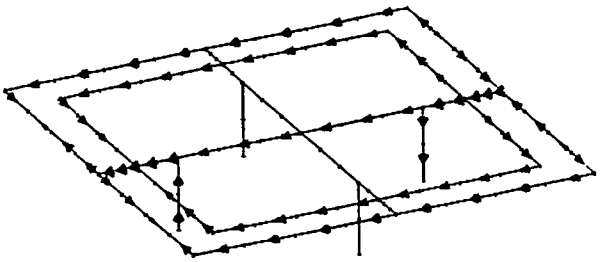

Fig. 2 Wire model of mesh antenna and its computed currents.

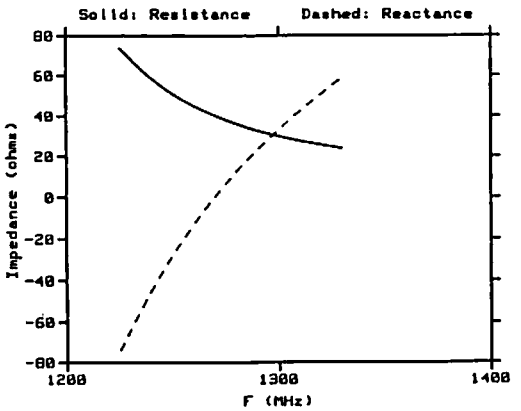

Fig. 3 Computed input impedance of the balanced feed.

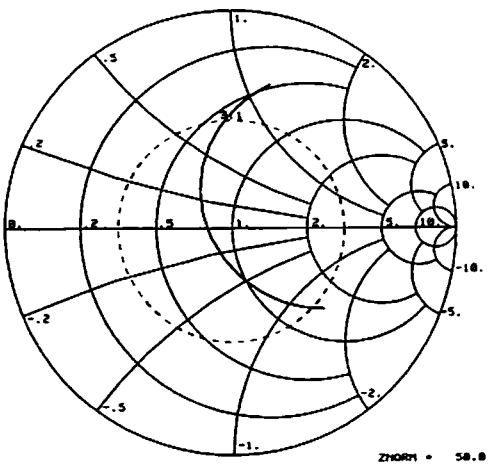

Fig. 4 Computed Smith Chart plot of the input impedance.

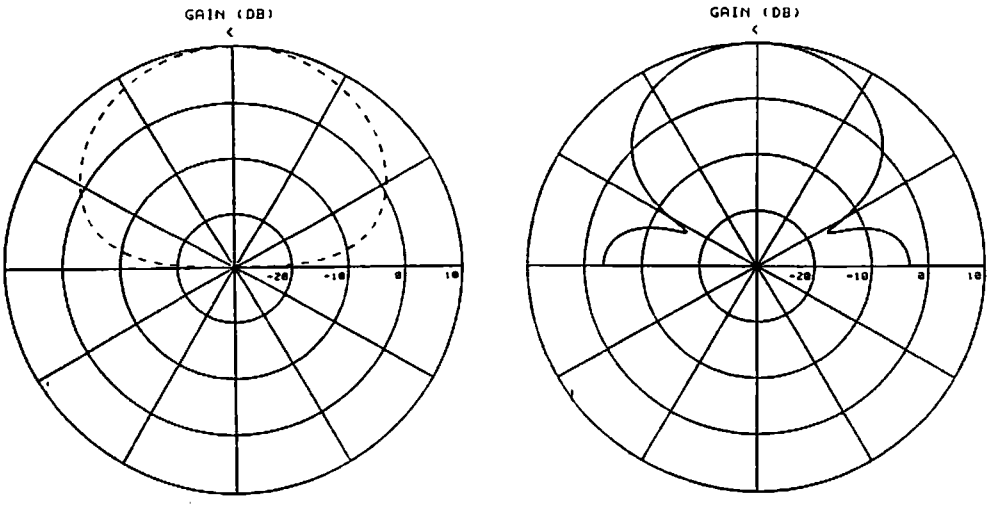

(a) (b)

Fig. 5 Computed radiation patterns of the antenna,
a) H-plane, b) E-plane

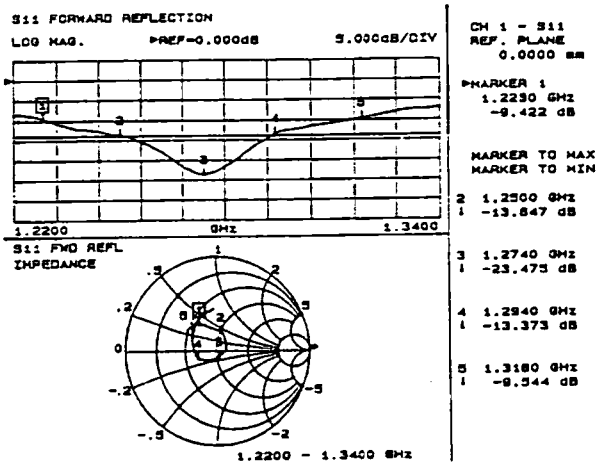

Fig. 6 Measured return loss S_{11} of the antenna